Aerosols in northeast Arabian Sea during the Indian winter monsoon: a study using sunphotometer measurements

Indrani Das*, A. K. Shukla and Mannil Mohan

Marine and Water Resources Group, Space Applications Centre, Ahmedabad 380 015, India

January is the month of the northeasterly monsoon over the Indian peninsula. Continental and anthropogenic aerosols are advected from the land to the ocean and mix with the marine atmosphere. This is an ideal time to study the dispersal of continental aerosols into the marine atmosphere.

This communication presents the results of the sunphotometer-measured aerosol optical depth (AOD) onboard *Sagar Kanya* over the northern Arabian Sea on its 186th mission, from 3 to 20 January 2003. The temporal, spectral and spatial variations of AOD are investigated. Relationship between AOD and relative humidity and variations in AOD and the Angstrom exponent from coastal to far-coastal regions of the ocean with respect to the prevailing wind conditions has been presented.

ALTHOUGH aerosols are minute particles, their cumulative effect on the atmosphere is tremendous. They can scatter away and absorb the incident solar radiation leading to cooling of the earth's surface and a simultaneous warming of the lower atmosphere[1–3]. Besides this direct radiative effect, aerosols act as condensation nuclei in the formation of clouds, which in turn scatter and absorb the solar and terrestrial radiations. The number density, chemical composition and size distribution can influence the lifetime of clouds and the rate of precipitation. Aerosols also pollute the atmosphere and reduce visibility[4,5].

Continental aerosols are mainly wind-blown mineral dust and carbonaceous and sulphate particles produced by forest fires, land use and industrial activities[6], while marine aerosols are mainly sea-salt particles produced by wave-breaking and sulphate particles produced by the oxidation of dimethyl sulphide released by the phytoplankton[7].

As the oceans cover more than 70% of the earth's surface, they are one of the largest sources of natural aerosols. Being hygroscopic, marine aerosols are crucial in cloud formation in the marine boundary layer and are also important in the radiative coupling between the ocean and the atmosphere. While continental aerosols can be both scattering and absorbing, marine aerosols are mostly of scattering type[8]; thus becoming a decisive factor in the albedo of the earth.

*For correspondence. (e-mail: dindrani_10@yahoo.com)

In spite of the ever-widening recognition of the direct and the indirect radiative effects of aerosols[9], they are still poorly characterized in climate models due to the lack of global information on their physical properties and spatial and temporal distributions.

During the months of December–February, northeasterly winds of the Asian winter monsoon carry aerosols from the Indian subcontinent and south Asian region[10] towards the pristine oceanic atmosphere of the southern hemisphere. These months therefore become an ideal period to study the effect of continental aerosols on the southern marine atmosphere.

Regular observations of aerosols have been carried out from the Minicoy island (8.3°N, 73.04°E) in the Arabian Sea[11] by making spectral extinction measurements in the visible and near infrared regions. The aerosol optical depth (AOD) over this region was found to have seasonal variations with an annual low in December–January and a high during July. To study the transport of continental aerosols into the marine atmosphere and to assess its effect on the radiation budget of the earth[12–15], a large number of observational campaigns have been conducted over the Arabian Sea and the tropical Indian Ocean during the Indian Ocean Experiment (INDOEX) and Aerosol Characterization Experiment (ACE project of ISRO-Geosphere Biosphere Programme). High concentrations of anthropogenic continental aerosols have been observed during January–March, north of the equator, which stay in the atmosphere till the summer monsoon washes them down[13–15]. A sharp decrease in AOD was observed at smaller wavelengths (~ 500 nm) from the northern hemisphere to the southern hemisphere south of ITCZ (Inter Tropical Convergence Zone), but a smaller decrease in AOD was observed at longer wavelengths (~ 1025 nm), which has been attributed to a predominance of submicron particles over the Arabian Sea in comparison with the southern oceans[15].

The AOD values were found to stabilize at distances ~ 1000 km from the shore and the columnar size distributions indicated a bimodal distribution[16,17]. In the deep oceans, AOD was found to have a good correlation with the wind speed, with AOD increasing exponentially for increasing wind speed. The spectral variation of AOD represented by the Angstrom exponent α, was found to be 0.97 ± 0.23 and 0.50 ± 0.30 in the near coastal and the far coastal regions respectively[18]. Relatively large values of α found in the near coastal regions indicate a greater amount of smaller particles in comparison with the far coastal regions[16]. High optical depths have also been observed in the central Arabian Sea (8 to 13°N; 57 to 65°E) far away from the coast[15], which has been attributed to aerosols brought to these regions by different air trajectories from South Africa, Arabian land mass and Southeast Asia.

Measurements and chemical analysis during the INDOEX have shown the Indo-Asian haze spreading in the north Indian Ocean consisting of inorganic and carbonaceous particles, including black carbon clusters, fly ash and mine-

ral dust[19]. Back-trajectory analyses have shown two different sources for aerosols over the Arabian Sea. One air mass travels from Saudi Arabia and Iran/Iraq to reach the Arabian Sea, while the other travels from Pakistan through the Indian coast of Gujarat, passing the Thar desert and Rann of Kutch[20].

In spite of a number of aerosol campaigns conducted in the oceans around India, few have been in the northern Arabian Sea (particularly, north of ~ 15°N), that too in the month of January. The present work is an effort to investigate the temporal, spectral and spatial variations of marine AOD over the northeastern Arabian sea based on the measurements taken on-board a research ship with reference to wind conditions and relative humidity during January 2003.

The 186th cruise of *Sagar Kanya* started on 3 January 2003 from Goa and ended on 19 January at the same port (Figure 1). The cruise area was confined within the latitudes 15.1 and 22.85°N and longitudes 72.4 and 67.6°E. The primary objective of this cruise was to study the phytoplankton bloom that occurs every year in the northern Arabian Sea during the winter monsoon. The cruise track in the background of monthly averaged NCEP (National Centre for Environmental Prediction) re-analysis wind field of January 2003 is shown in Figure 1. Starting from Goa, the ship moved northwestwards into the ocean away from the coast and reached the northernmost point on 14 January. Then it returned to Goa on a track closer to the coast.

During the cruise, an EKO sunphotometer with five spectral channels centred around 368, 500, 675, 778 and 862 nm, was operated at every half an hour interval on cloud-free days. Simultaneous meteorological observations like wind speed and relative humidity were recorded by an automatic weather station and the atmospheric pressure was measured with an on-board aneroid barometer. In general, the days were cloud-free during most of the cruise period and a good dataset could be obtained.

The EKO sunphotometer design comprises of a collimating tube with a narrow field of view (~ 2.4°)[21], a series of five interference filters mounted on a rotating wheel and a solid-state detector connected to an amplifier and a voltmeter. Band-pass filters with ± 2 nm FWHM (full width at half maximum) bandwidth were used. Calibration of the instrument was done following the Langley plot method[12,22]. Data of three clear days, 9, 10 and 12 January in the far coastal ocean were used for this purpose, since the Langley plot technique is valid only under the condition of stable optical depth over the whole day. Figure 2 shows the Langley plot for 500 nm made from measurements on 10 January.

The calibration coefficients obtained from the Langley plots (after correcting for the solar flux changes due to the day-to-day change in sun–earth distance) were then averaged for each wavelength to obtain the standard calibration coefficients. These were then used to determine the total atmospheric optical depths (τ_{total}) for each of the measurements. The total atmospheric optical depth can be split into:

$$\tau_{total} = \tau_{Rayleigh} + \tau_{aerosol} + \tau_{ozone}, \quad (1)$$

where $\tau_{Rayleigh}$ is the optical depth due to Rayleigh scattering in the atmosphere, $\tau_{aerosol}$ is the optical depth due to aerosol scattering and absorption, and τ_{ozone} is the optical depth due to absorption by atmospheric ozone.

The values used for ozone optical depth (τ_{ozone}) for the five channels of the sun photometer are 0.0, 0.0114, 0.0144, 0.0 and 0.00 respectively[21,23].

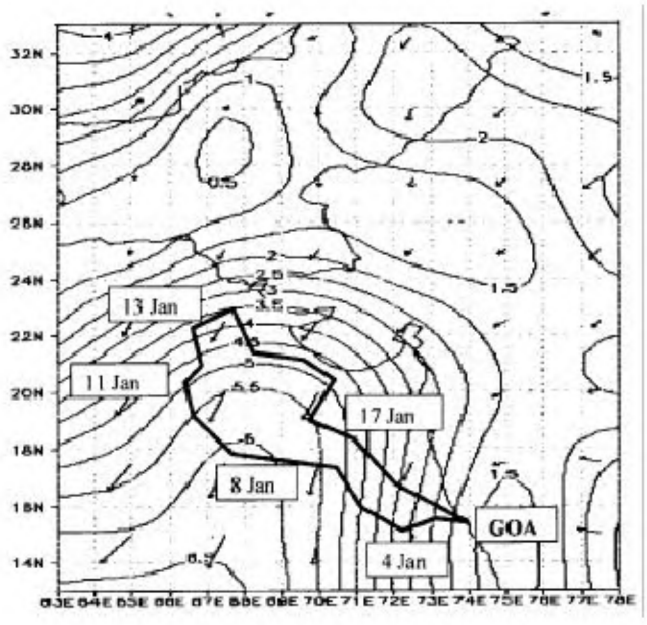

Figure 1. Cruise track of *ORV Sagar Kanya*, mission SK 186 superimposed on 1000 mb pressure level wind isotachs (m/s) averaged for the month of January 2003 from NCEP.

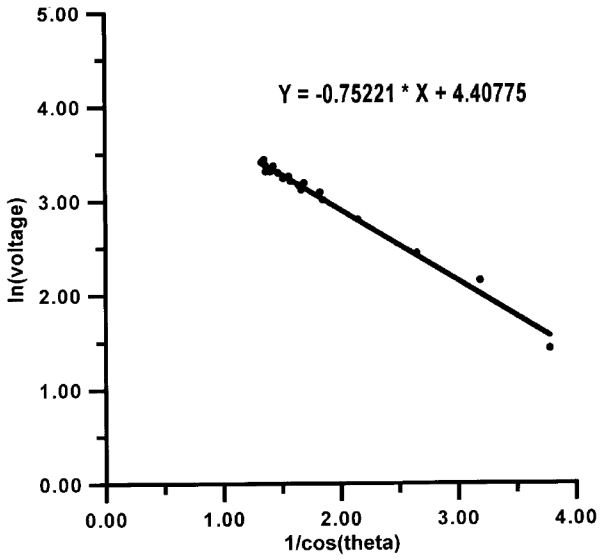

Figure 2. Typical Langley plot at 500 nm for 10 January 2003.

The Rayleigh optical depth was computed as[24]

$$\tau_{\text{Rayleigh}} = 0.00838 \times \frac{p_a}{p_0} (\hat{l})^{(-3.96+0.079\times\lambda+0.050\times\lambda)}, \quad (2)$$

where p_a is the prevailing atmospheric pressure, p_0 = 1013 mb (standard atmospheric pressure at the sea level), and λ is the wavelength in nm.

The AOD was then determined as

$$\tau_{\text{aerosol}} = \tau_{\text{total}} - \tau_{\text{Rayleigh}} - \tau_{\text{ozone}}, \quad (3)$$

which was then averaged for each day to obtain the daily AOD. The error in the determination of AOD was < 3%, arising from the standard deviations in the calibration coefficients and instrumental and measurement errors.

The average wind speed for the month of January in the cruise region ranged from 3.5 to 6 m/s and the direction of the wind was from the Indian land mass to the ocean, which was conducive to the transport of continental aerosols into the marine atmosphere.

The daily spectral AOD from 5 to 18 January 2003 is shown in Figure 3, where one can notice an overall decrease in the AOD from near coast (refer Figure 1) to far away from the coast. The spectral spread is more in the coastal regions than in the far-coastal regions. Similar to the observations reported earlier[15,18], this is due to the presence of smaller continental particles near the coast, whose influence diminishes towards the far-coastal regions which gets increasingly dominated by larger-sized marine aerosols.

Figure 4 shows the daily averaged relative humidity (RH). Comparison between Figures 3 and 4 shows that AOD has a nearly similar day-to-day variability as that of RH. Figure 5 is a scatter plot between AOD at 500 nm and RH, which has a correlation of 0.89. In other wavelengths, the correlation was between 0.87 and 0.92. Such good correlation could be resulting from the effect of RH on aerosol size[25]. Aerosols, acting as condensation nuclei, grow in size under high RH conditions, leading to larger scattering cross-sections and thereby to higher optical depth[19,26,27]. This process is also in agreement with the satellite observations on the growth of aerosols in a moist atmosphere leading to cloud formation[5].

The scatter plot in Figure 5 has the regression relation

$$\text{AOD} = 0.0159 * \text{RH} - 0.60306, \quad (4)$$

showing a negative AOD for RH ~ 0.0%, which we know is not possible. One can only explain that the curve starting with positive AOD at low RH becomes steeper in the RH range 45 to 65%. Or in other words, the AOD–RH relationship is nonlinear[26,27]. But in order to get the actual shape of the curve, measurements over a RH range 0 to 90% are needed, which were not available in this cruise.

Figure 6 shows examples of spectral AOD in the near-coastal waters (16 January) and in the far-coastal regions (9 January). Assuming an Angstrom power law[5], a best-fit curve was fitted to the spectral AOD of each day and the Angstrom exponent was determined. The value of the exponent as a function of distance from the coast is shown

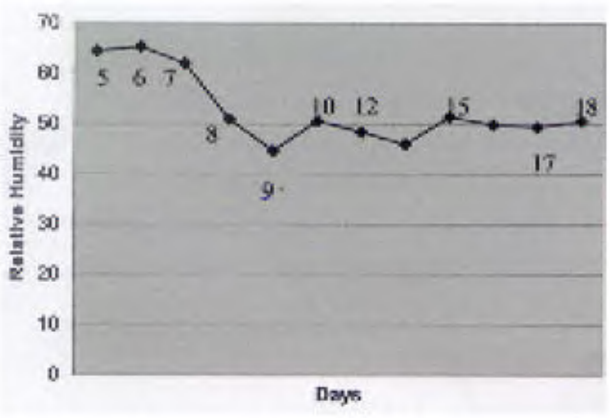

Figure 4. Variation of daily averaged relative humidity corresponding to those days when AOD was measured.

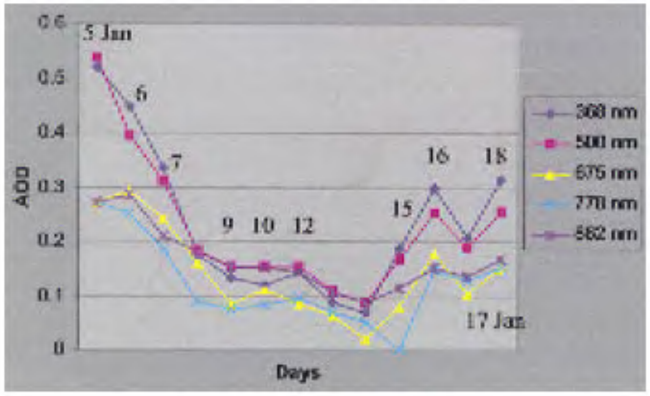

Figure 3. Spectral variation of AOD for all the clear days of the cruise. The spectral spread becomes less towards the open ocean.

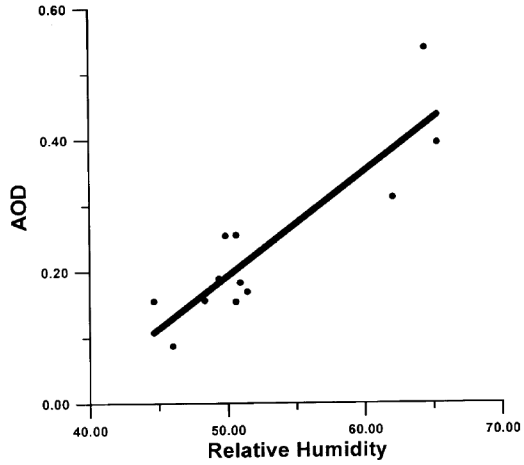

Figure 5. Scatter plot of daily averaged relative humidity versus daily averaged AOD at 500 nm, showing a correlation of 0.89.

in Figure 7. The distance of each point on the track from the land was measured in the direction of the prevailing wind, which has remained nearly constant (~ north northeast, shown in Figure 1) throughout the cruise period. The farthest point on the track from the coast was ~ 470 km.

The value of the Angstrom exponent decreased from ~ 0.79 ± 0.12 in the near-coastal regions (< 150 km from mainland) to ~ 0.40 ± 0.25 in the far coastal regions (~ 470 km from mainland), as shown in Figure 7. Since the Angstrom exponent is oppositely related to the average size of the aerosols[5], an increase in its value will mean the prevalence of smaller particles and vice versa. Coastal atmosphere is mainly infiltrated by aerosols from land, which are smaller in size compared to their marine counterpart[12].

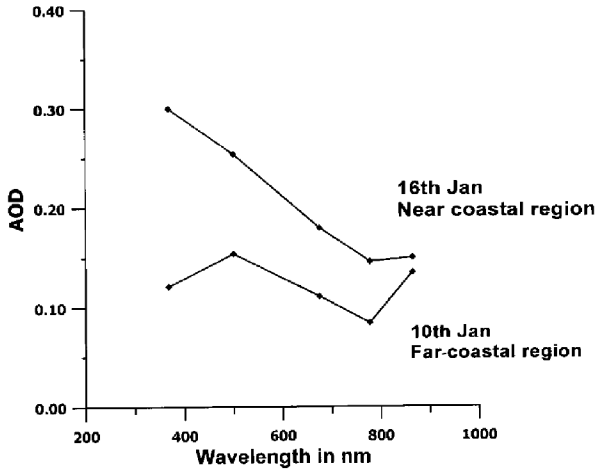

Figure 6. Spectral variation of AOD on 16 January when observations were taken in near-coastal waters and on 9 January when the ship was in the far-coastal regions.

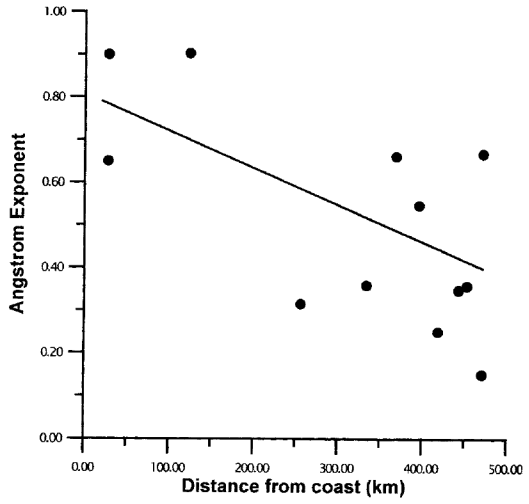

Figure 7. Value of the Angstrom exponent as a function of distance from the coast.

The temporal, spatial and spectral variations of AOD in the northeastern Arabian Sea and its relationship to RH and wind speed are studied using sunphotometer measurements collected on-board *ORV Sagar Kanya* during its 186th cruise from 3 to 20 January 2003. The following conclusions can be drawn from this study.

(i) There is an overall decrease in the AOD from near-coast to far-coastal regions.
(ii) There is a good correlation between the daily averages of AOD and the RH. The negative y-intercept in the regression curve indicates a nonlinear relationship.
(iii) The value of α in the near-coastal regions decreased from 0.79 ± 0.12 to 0.40 ± 0.25 in the far-coastal regions, indicating that the average aerosol particle size increased from the coast towards far-coastal regions.

1. Coakley, J. A., Cess, R. D. and Yurevich, F. B., The effect of tropospheric aerosols on the earth's radiation budget: A parameterisation for climate models. *J. Atmos. Sci.*, 1983, **40**, 116–138.
2. Charlson, R. J., Schwartz, S. E., Hales, J. M., Cess, R. D., Coakley, J. A., Hansen Jr. J. E. and Hofmann, D. J., Climate forcing by anthropogenic aerosols. *Science*, 1992, **255**, 423–430.
3. Kaufman, Y. J. *et al.*, Passive remote sensing of tropospheric aerosol and atmospheric correction for the aerosol effect. *J. Geophys. Res.* 1997, **102**, 16,815–16,830.
4. Das, I., Mohan, M. and Krishnamoorthy, K., Detection of marine aerosols with IRS P4-Ocean Colour Monitor. *Proc. Indian Acad. Sci. (Earth Planet. Sci.)*, 2002, **111**, 425–435.
5. Das, I. and Mohan, M., Detection of marine aerosols using ocean colour sensors. *Mausam*, 2003, **54**, 327–334.
6. Penner, J. E. *et al.*, Quantifying and minimizing uncertainity of climate forcing by anthropogenic aerosols. *Bull. Am. Meteorol. Soc.*, 1994, **75**, 375–400.
7. Charlson, R. J., Lovelock, J. E., Andreae, M. O. and Warren, S. G., Oceanic phytoplankton, atmospheric sulphur, cloud albedo and climate. *Nature*, 1987, **326**, 655–661.
8. D'Almeida, G., Koepke, P. and Shettle, E., *Atmospheric Aerosols: Global Climatology and Radiative Characteristics*, A. Deepak, Hampton, Va., 1991, p. 561.
9. Intergovernmental Panel on Climate Change, Report to IPCC from Scientific Assessment Group (WGI), Cambridge University Press, New York, 1995.
10. Satheesh, S. K. and Ramanathan, V., Large differences in tropical aerosol forcing at the top of the atmosphere and earth's surface. *Nature*, 2000, **405**, 60–63.
11. Krishna Moorthy, K. and Satheesh, S. K., Characteristics of aerosols over a remote island, Minicoy in the Arabian Sea: Optical properties and retrieved size characteristics. *Q. J. R. Meteorol. Soc.*, 2000, **126**, 81–109.
12. Satheesh, S. K., Krishnamoorthy, K. and Das, I., Aerosol spectral optical depths over the Bay of Bengal, Arabian Sea and Indian Ocean. *Curr. Sci.*, 2001, **81**, 425–435.
13. Jayaraman, A., Results on direct radiative forcing of aerosols obtained over the tropical Indian Ocean. *Curr. Sci.*, 1999, **76**, 924–930.
14. Jayaraman, A., Aerosol radiation cloud interactions over the tropical Indian Ocean prior to the onset of the summer monsoon. *Curr. Sci.*, 2001, **81**, 1437–1445.
15. Krishna Moorthy, K., Saha, A., Prasad, B. S. N., Niranjan, K., Jhurry, D. and Pillai, P. S., Aerosol optical depths over peninsular India and adjoining oceans during INDOEX campaigns: Spatial, temporal

and spectral characteristics. *J. Geophys. Res. D*, 2001, **106**, 28,539–28,554.
16. Krishna Moorthy, K., Satheesh, S. K. and Krishna Moorthy, B. V., Investigations of marine aerosols over the tropical Indian Ocean. *J. Geophys. Res. D*, 1997, **102**, 18,827–18,842.
17. Krishna Moorthy, K., Satheesh, S. K. and Krishna Moorthy, B. V., Characteristics of spectral optical depths and size distributions of aerosols over tropical oceanic regions. *J. Atmos. Sol. Terr. Phys.*, 1998, **60**, 981–992.
18. Satheesh, S. K. and Krishna Moorthy, K., Aerosol characteristics over coastal regions of the Arabian Sea. *Tellus*, 1997, **B49**, 417–428.
19. Ramanathan, V. *et al.*, Indian Ocean Experiment: An integrated analysis of the climate forcing and effects of the great Indo-Asian haze. *J. Geophys. Res. D*, 2001, **106**, 28,371–28,398.
20. Ramachandran, S. and Jayaraman, A., Premonsoon aerosol mass loading and size distribution over the Arabian Sea and the tropical Indian Ocean. *J. Geophys. Res. D*, 2002, **107**, 4378.
21. *EKO Sunphotometer Instruction Manual*, 2000, p. 3.
22. Krishna Moorthy, K., Nair, P. R. and Krishna Moorthy, B. V., Multi-wavelength solar radiometer network and features of aerosol spectral optical depth at Trivandrum. *Indian J. Radio Space Phys.*, 1989, **18**, 194–201.
23. Jayaraman, A., Lubin, D., Ramachandran, S., Ramanathan, V., Woodbridge, E., Collins, W. D. and Zalpuri, K. S., Direct observations of aerosol radiative forcing over the tropical Indian Ocean during the January–February 1996 pre-INDOEX cruise. *J. Geophys. Res. D*, 1998, **103**, 13827–13836.
24. Doerffer, R., Imaging spectroscopy for detection of chlorophyll and suspended matter. GKSS 92/E/54, GKSS-FORSCHUNGSZENTRUM GEESTHACHT GMBH, 1992.
25. Hanel, G., Parameterization of the influence of relative humidity on optical aerosol properties. *Aerosol and their Climatic Effects* (eds Gerber, H. E. and Deepak A.), A. Deepak Publishing, 1984, pp. 117–122.
26. Tomasi, C., Non selective absorption by atmospheric water vapour at visible and near infrared wavelengths. *Q. J. R. Meteorol. Soc.*, 1979, **105**, 1027–1040.
27. Nair, P. and Krishna Moorthy, K., Effects of changes in atmospheric water vapour content on physical properties of atmospheric aerosols at a coastal station. *J. Atmos. Sol. Terr. Phys.*, 1998, **60**, 563–572.

ACKNOWLEDGEMENTS. We are grateful to the ISRO-Geosphere Biosphere Programme for financial support. We thank Mr R. M. Dwivedi and the team members of SK 186 mission for their kind co-operation during the period of the cruise. We also express our gratitude to the anonymous referees for their comments and suggestions to improve the manuscript.

Received 1 August 2003; revised accepted 3 December 2003

Estimation of ground insolation using METEOSAT data over India

S. Kimothi[1], B. K. Bhattacharya[2], P. D. Semalty[1], V. K. Pandey[2] and V. K. Dadhwal[2,*]

[1]Department of Physics, S.R.T. Campus College, Badshahi Thaul, H.N. Bahuguna Garhwal University, Srinagar 249 199, India
[2]Crop Inventory and Modelling Division, Agricultural Resources Group, Space Applications Centre (ISRO), Ahmedabad 380 015, India

Ground insolation or short-wave incoming radiation (SWR) at the ground is an important input in models of vegetation productivity, hydrology, ecological functioning, crop growth, etc. but is measured over limited number of stations, which fail to capture its spatial variability. A physical retrieval scheme was used for mapping insolation using METEOSAT VISSR sensor data over the Indian landmass for the winter season. The analysis covered the months of November–December 1998 and January 1999, and used five daytime acquisitions of meteosat visible (0.3–1.1 μm), thermal (10.5–12.5 μm), water vapour (6.5–7.5 μm) channel data. A total of 450 images per band per month was processed to retrieve instantaneous, daily total and five-day average total SWR over India. The estimated SWR was compared with the ground-measured pyranometer data over 18 Indian land stations acquired from India Meteorological Department. This validation for instantaneous SWR at 10:00 and 14:00 h, and daily total SWR for six selected dates (1, 5, 10, 15, 20, 25) of each month indicated root mean squared error (RMSE) of 62.51–91.93 Wm^{-2}, i.e. 15–18% of observed mean and 1.14–1.74 MJm^{-2} respectively. When five-day averages for the three-month period were compared, METEOSAT-derived data had a RMSE of 1.93 MJm^{-2}, which is 12% of the mean over pooled data.

THE short-wave incoming radiation (SWR) or insolation received at the ground surface is one of the important inputs to energy–water models, ecological modelling, global climate-change studies, crop-simulation model and models for estimating net primary production (NPP). Ground-based measurements of insolation are generally made with pyranometers or with measurement of duration of sunshine at weather stations. These stations are too sparse to capture spatial variability of SWR. Because of the strong modulation of insolation by clouds, use of RS data is an ideal approach for routine regional mapping of SWR. While use of polar orbiting satellites with sensors such as ERBE[1] having broad visible band or NOAA AVHRR[2,3], Landsat TM[4] with multispectral bands has been made for insolation, it is the geostationary platform that provides multiple passes everyday, ideal for such an application. A

*For correspondence. (e-mail: vkdadhwal@sac.isro.org)